NUMERICAL SIMULATION OF THE FORMATION AND

REATACHMENT LENGTH OF WATER JET FOR DIFFERENT

ORIFICE GEOMETRIES

Amanuel T. Basha, Massimiliano Annoni, Michele Monno
Politecnico di Milano
Dipartmento di Meccanica
Milan, Italy

ABSTRACT

The flow through water jet orifices is important because of its effects on the jet characteristics (jet break-up length and momentum distribution). In this paper, Computational Fluid Dynamics (CFD) simulation was performed to improve the understanding of water jet formation and fluid flow process through the orifice under high injection pressures. In particular, water jet formation and reattachment length in sharp edged diamond orifices were studied. The investigation used a two dimensional, axisimetric, two-phase, transient-state model of orifice flow to observe the effects of capillary length and diameter on the jet break-up length. The injection pressure was varied from 10 MPa to 700 MPa. Results are presented for two standard diamond orifice types. Type-1 orifice, which is used for pure water jet cutting, produced a constricted water jet with no apparent cavitations during the jet formation at typical water jet cutting pressures. On the other hand, flow in type-2 orifice (a typical orifice used for abrasive water jet cutting), at similar injection pressures, quickly reattaches to the wall of the orifice.

1.INTRODUCTION

Abrasive Water jet (AWJ) cutting has a great potential of being an effective and sustainable manufacturing technology. Some advantages are clean cut edges, high accuracy and flexibility, low material loss, inert and relatively abundant main processing substances (water, garnet) and negligible thermal influence on the work piece.

The use of the abrasive water jet for machining or finishing purposes is based on the principle of erosion of the target material. The efficiency and accuracy with which the material is cut depends mainly on the peculiar characteristics of the employed high-speed water jet. One of the requirements for efficient and accurate cutting by the water jets is to maintain their kinetic energy for a certain distance downstream the orifice, thus providing jets with high intact lengths (also called break-up lengths).

Orifices are one of the fundamental devices in fluid mechanics. Small, high-speed liquid jets are used in numerous industrial applications such as engines and water jet cutting. In the case of water jet cutting, orifices are critical for creations of energetic jets capable of efficient and accurate cutting. Unfortunately, very little knowledge is available about the internal flow through high pressure injector orifices. In industrial jet machining, injection pressures easly exceed 150 MPa with orifice diameters on the order of 150-400 microns. The internal nozzle flow can reach speeds up to 900 m/s. This combination of high speed and small size makes experimental measurements of the flow extremely difficult. The orifice flow cannot be easily scaled up for experimental study, because the flow is described by a large number of parameters, many of which involve fluid properties.

The role of orifice geometry on the formation of liquid jets has been discussed extensively in the literature. Recent experimental studies by Akira *et al* [1], Tamaki *et al* [2] and Hiroyasu [3] show that the occurrence of cavitation inside the orifice makes substantial contributions to the break-up of the exiting liquid jet. The collapse of cavity bubbles can increase the disturbances in the flow leading to a faster break-up of the jet. Even with high pressure drops, the main flow of the liquid jet does not atomize greatly when disturbances caused by cavitation are not present [1]. Tafreshi and Pourdeyhimi [4] carried out a numerical simulation on cavitation and hydraulic flip inside hydroentangling nozzles. They showed that, under certain conditions, cavity extends to the orifice exit and results in hydraulic flip. When hydraulic flip occurs, cavitation vanishes due to the fact that downstream air moves upward into the nozzle. This leads to the elongation of the jet break-up length. Chaves [5] obtained photographs and made some measurements in small, cavitating nozzles and also looked at the subsequent sprays. N. Anantharamaiah et al [6] studied flow simulations of water through sharp-edged cone-capillary nozzles at different Reynolds numbers (less than 20 MPa). The simulations showed the separation of the flow from the nozzle wall as it enters the orifice. Their simulations have also revealed that flow reattachment occurs in cases where the nozzle capillary length is longer than a critical length. For sharp-edged nozzles operating at moderate Reynolds numbers (up to 30000), they reported the critical capillary length to be about 70% of the considered nozzle diameter. They argued that nozzles with a capillary length less than this critical length produced a constricted water jet with no apparent cavitation during the jet formation.

The characteristics of water jets strongly depend on the injection pressure [7]. The water jets used in cutting applications are distinct by their high injection pressures (150 MPa-to-400 MPa). Therefore, extending the discussion in literature on the flow through water jet orifices is appropriate. For improving our understanding of the flow inside a water jet orifice at real Reynold's numbers (more than 60000), CFD analysis is found to be a viable approach because direct measurement and visualization of pure water velocity distributions are very difficult for the high Reynold's number and small dimensions involved. In this paper, CFD simulation for jets at high Reynolds number (up to 170000) in small orifices (150 and 250 microns) is performed using the Fluent CFD solver. Jet dynamic characteristics such as the pure water velocities and reattachment length in a water jet orifices are then simulated under unsteady state, turbulent, two-phase (air and liquid) flow conditions, and at range of injection pressures. The results of the CFD study are then analyzed to gain insight into the jet characteristics. A further understanding was established for efficient cutting with high velocity water jets considering the variations in length to diameter ratio of the orifice capillary. In the study, it is concluded that the critical reattachment length to avoid cavitation in water jet cutting varies with the diameter and increases with the injection pressure.

1.1 Water Jet orifices

The heart of the water jet process is the orifice (Fig. 1). Water jet orifices have to create coherent jets. Such a behaviour can only be achieved through the proper design of their internal geometries, where the different non-dimensional geometric variables must remain within a well-specified range during the useful lifetime of the orifice [8].

Typical industrial water jet orifices have cone-capillary configurations (Fig 1: the main reason for may be the ease of manufacturing a conical hole across the 0.5 mm thickness of the sapphire/diamond, compared to a completely cylindrical hole. Although a purely conical shape would suffice, the orifice inlet of such a nozzle would deteriorate at a faster rate under such high operating pressures. Thus, the cylindrical (capillary) portion of the nozzle on top of the conical configuration would provide a mechanically stronger inlet edge [8]. The uniformity of the product and the repeatability of the cutting process require a continuous and locally uniform jet-material interaction. It is important that the water jets maintain their kinetic energy downstream the orifice for an appreciable distance. However, in nature water jets break-up dividing their kinetic energy among thousands of very fine droplets. Broken water jets tend to become practically ineffective and consequently not able to cut materials efficiently and accurately.

Studies over the years have pointed out that the break-up properties of the jet are influenced by a large number of parameters. These are mainly hydrodynamic forces (surface tension forces, internal forces, viscous forces and initial disturbances) in the liquid jet, aerodynamic interaction effects and nozzle internal flow effects resulting from cavitation and the flow separation inside the nozzle, jet velocity profile rearrangement effects and liquid turbulence at the nozzle exit [9,10,11,12,13]. Among the parameters that are known to affect water jet break up length, many are associated with the nozzle non-dimensional geometric parameters [8, 9].

Water jets for cutting are issued from tiny orifices made of sapphire or diamond in a metallic housing (see Figure 1). Manufacturing of such delicate tiny orifices places constraints on the

design process. Typically, industrial jet orifices have a thickness L_t of about 0.5 mm, and a typical orifice Aspect Ratio $AR \approx 1$ (ratio between the length of the capillary portion and the inlet diameter). The performance of water jet orifices depends not only on their nominal diameter but also on their internal geometry, which means inlet roundness, length of the capillary section, length and angle of the cone section, ratio of the inlet roundness to diameter, ratio of the length of the cylindrical section to diameter and so on [14]. The effect of these non-dimensional ratios on the cutting performance and, in particular, the effect of the position of the cone section, (cone-up orifices: cone section at the entrance; cone-down orifices: cone section at the exit) were experimentally studied at the water jet lab of the departmento di Meccanica of the Politecnico di Milano [14].

Orifice separates a high pressure body of water from the downstream air; flow may detach from the wall and form a vena-contracta (necking) when it enters the capillary. Depending on the length of the capillary and the hydrodynamic conditions, this flow may or may not reattach to the wall after some distance [6]. In the case of detached flows, there is an air gap between the liquid and the capillary wall. This air envelops the flow all the way through the capillary and does not allow any contact between liquid phase and the capillary wall. As a result, wall-induced friction and cavitation do not disturb the structure of this flow. Detached flows have peculiar characteristics that are particularly useful for water jet cutting applications. A water jet resulted from a detached flow, the so-called constricted water jet [6], has a higher stability and, therefore, a longer break up length [3,6,8]. The constricted water jets stay laminar even at remarkably high Reynolds numbers such as in the case of water jets cutting applications, in contrast to the non-constricted water jets. Constricted jets are therefore formed when the water flow enters the capillary section of the cone-capillary orifice and the jet is detached either because of non-dimensional geometric parameters (hydrodynamic conditions) in the orifice or due to the orifice undergoing hydraulic flip. The non-constricted jet is formed when water enters the nozzle from the conical side or when reattachment without hydraulic flip occurs in a cone down configuration.

It is important to note that the discharge coefficient of a nozzle, defined as the ratio of the real (experimental) flow rate to the flow rate calculated by using the Bernoulli equation and the nominal cross-section area, is about 0.62 and 0.92 depending respectively on whether the flow is detached or not [6,15].

1.2. The considered orifices

In the present study, we simulated the water flow through two standard sharp-edged diamond orifices: type -1 and type-2 orifices (geometric characteristics are shown in table 1). Type-1 orifice is used for pure water jet cutting applications therefore, the exiting jet shows a more coherent and long break-up length. Whereas, the type-2 orifice is used for AWJ applications where higher discharge coefficient is achieved for better mixing with abrasive particles and consequently for better cutting. The orifices in this study are all cone-down orifices [14] and they can be considered as sharp-edged since they can count on an inlet roundness close to zero, thanks to the properties of diamond.

2-NUMERICAL SIMULATION

The numerical solution of the governing Navier-Stokes equations of incompressible, unsteady, axisymmetric flow is performed using the finite-volume (Patankar, 1980) method [16] on a staggered grid; and the best convergence was achieved with PISO algorithm [17] for coupling the pressure and velocity fields. In the finite volume method, the solution domain is subdivided into a large number of control volumes. The governing partial differential equations are integrated over these control volumes and converted into their algebraic equivalents. The obtained set of algebraic equations is then solved by iterative methods. Presto scheme was employed for discretisation of the pressure equation and the second order upwind for the rest of continuum equations.

The employed two-phase flow solution method used is the Volume Of Fluid (VOF) [18] implemented in Fluent 6. A single momentum equation is solved throughout the domain resulting in a velocity field shared among liquid and air. The calculation is done for Reynolds numbers greater than 60000.

Liquid water enters the solution domain from a pressure inlet boundary. The outgoing flow leaves the domain from a pressure outlet boundary. Flow properties are assumed to be constant across the boundaries. For this reason, the boundaries are placed far (at 5 times the capillary diameter) from the capillary section, region under investigation, where strong gradients are expected. For the flow simulation close to solid boundaries, no-slip boundary condition was assumed. The computational domain is shown in Figure 2.

2.1 Governing Equations

In this study, we consider the water flow through the two types of orifices (see Table 1) the resulting exiting jet into a stagnant air. The physical problem the computational domain and grid are shown in figure 2. Governing equations for an unsteady, incompressible viscous flow are the Navier-Stokes equations:

Continuity equation:

$$\frac{\partial \rho}{\partial t} + \nabla \cdot (\rho \bar{v}) = 0 \tag{1}$$

Momentum equation:

$$\frac{\partial (\rho \bar{v})}{\partial t} + \nabla \cdot (\partial \bar{v} \bar{v}) = -\nabla p + \nabla \cdot \mu (\nabla \bar{v} + \nabla \bar{v}^T) + \rho \bar{g} + \bar{F} \tag{2}$$

To track the interface between the phases, a volume fraction continuity equation for liquid phases is solved along with the above equations.

$$\frac{\partial \alpha_q}{\partial t} + \bar{v} \cdot \nabla \alpha_q = 0 \qquad (3)$$

The properties appearing in the transport equations are determined by the presence of the component phases in each control volume. density, for example, is considered to be:

$$\rho = \sum_{q=1}^{2} \alpha_q \rho_q \qquad (4)$$

The geometric reconstruction scheme [19] was used as it showed the highest accuracy in predicting the interface. The surface tension is included in the calculation, though these forces are negligible at high velocities. The surface tension model in Fluent is the continuum surface force (CSF) model [20]. With this model, the surface tension is written in terms of a pressure jump across the surface. The force at the surface is expressed as a volume force and is added to the momentum equation as a source term. In Fluent, the surface curvature, κ, is computed from local gradients in the surface normal at the interface:

$$\kappa = \nabla \cdot \hat{n} \qquad (5)$$

where,

$$\hat{n} = \frac{n}{|n|} \text{ and } n = \nabla \alpha_q \qquad (6)$$

The above scheme results in the prediction of the water-air interface in the whole domain, which is the main purpose of this study.

All the discussed simulations are transient state with time steps in the nanosecond range. Having small time steps is essential for reaching convergence in each time step at this but it makes the simulations time consuming. The convergence criteria for these simulations are defined in terms of "residuals". The residuals provide a measure of the degree of satisfaction of each of the conservation equations throughout the flow field. The residual for each flow variable gives a measure of the error magnitude in the solution in iteration. A three orders of magnitude reduction in the residuals is normally required for a solution to be considered converged [17]; this case has to be achieved in all simulations.

2.2. Grid independence

The grid independency of the solution was investigated for flow with $Re = 116190$ ($p= 300$ MPa), by increasing the number of grid points by 50 % in the axial and radial directions. Figure 3 shows water frontline for the above mesh densities after 120 nanoseconds for 40 x 80, 80 x 160 and 160 x 320 mesh densities in the capillary of type -1 orifice. It can be seen that increasing the mesh density results in a more distinct interface; however the overall shape of the liquid front is

not remarkably changed. For this reason, and to reduce the computation time, the intermediate mesh density, 80 × 160, was chosen for the rest of our calculations.

3-RESULTS AND DISCUSSIONS

In this section, simulation results aimed to calculate the flow reattachment length inside the orifice are reported. To determine whether a flow through a passage is laminar or turbulent, the Reynolds number, defined basing on the capillary diameter, is compared to a value of about 2300, above which the flow is considered to be turbulent. Such a definition is based on the assumption that the water flow is in contact with the passage walls and turbulence is induced into the flow by wall friction. In cases where flow is detached and is in contact with air rather than wall, the degree of turbulence induced to the stream is significantly less. It is known from the literature that detached flows remain laminar for a wide range of velocities [8]. For this reason, a laminar model was considered for all simulations. When the flow reattaches the simulation faces instabilities and are interrupted ones the flow reattaches to the wall. Because the main focus of this study is to observe the reattachment length for different conditions. Reynolds number based on capillary diameter,

$$R_e = \frac{\sqrt{2\rho p}\, d}{\mu}\,,$$ (7)

 is reported but only for comparison between different simulations and/or experimental data.

3.1 Validation of the numerical solution

The real geometry for representing a water jet orifice has the geometric characteristics shown in Table 1. Inlet corner can be considered sharp (few microns). We have chosen type-1 orifice with as a starting point to allow for comparison to available experimental data. Usually nozzle experiments are run with an atmospheric downstream pressure and a variable upstream pressure. We have performed calculations at upstream pressures from 10 MPa up to 700 MPa. We have fixed the downstream pressure as atmospheric. Conducting experiments for validating the simulation data for the cases discussed here is difficult. In this case, the parameter that can be used for validating the simulation results is the discharge coefficient. The nozzle discharge coefficient were calculated from simulations. Discharge coefficient (Equation 8), by definition, is the ratio of the actual (experimental) flow rate to the flow rate obtained for an ideal flow (from Bernoulli equation). Simulated discharge coefficient, on the other hand, is the ratio of the mass flow rate obtained from viscous flow numerical simulation to that extracted from the in viscid theory (from Bernoulli equation).

$$C_d \equiv \frac{\dot{m}}{A\sqrt{2\rho(p_0 - p_1)}}$$ (8)

The discharge coefficients were measured at a distance of 60 micrometers downstream the inlet during the jet formation (unsteady-state condition). The discharge coefficients for type-1 orifice

were found to be about 0.61 and stayed the same until the steady-state condition was reached. This value is in good agreement with the results of experimental studies on steady-state constricted water jets [15, 21, and 22]. However, the discharge coefficient in the type-2 orifice, changed from about 0.61 to 0.93 with time as the fluid flowed through the capillary (unsteady-state condition). This condition indicates flow reattachment which can be followed by orifice cavitations [19]. The results of the discharge coefficient for both orifice types are consistent with their application: it is favourable to have more coherent and long break-up length jet for type-1 orifice for pure water jet cutting. And it is also favourable to have higher discharge coefficient for orifice type-2 used in AWJ cutting as better mixing with the abrasive particles is achieved.

As another validation of the employed model, we have compared the predicted centerline velocity to the measured velocity in [14] ; the geometry of the orifice tested are similar to the simulated orifices. We have also compared to values suggested by Chaves [5]. Chaves measured the centreline velocity of cavitating nozzles, performed the experiments with an atmospheric downstream pressure. He found that the measured velocities were approximately equal to the Bernoulli velocity. In Figure 4, the numerical predictions of centreline velocity for type-1 orifice are shown along with the experimental data from [14] and the value suggested by Chaves. The numerical results agree closely with correlation of Chaves [5]. The apparent difference the simulation and the experimental results from [14] may be due to the difference in the position of the measurement point along the jet axis. For the experiment in [14], Laser beams of the employed laser Doppler velocimetry have been focused on the jet axis at a distance of about 22 mm from the exit of the diamond orifices. Along this distance, the jet might have lost velocity due to the interaction with ambient air. The fact that the simulation closely predicts the bulk mean velocity as measured by the coefficient of discharge and the velocity at the centreline suggests that the exit velocity profile is essentially correct. An important feature of these two quantities is that the centreline velocity is approximately equal to the bulk mean velocity. This means that the exit velocity profile is flat, as one would expect for detached laminar flows. The common uniform velocity assumption of nozzle exit flow appears to be valid for cavitation-free detached flow in orifices at high injection pressures of water jet cutting.

3.2 Flow in water jet orifice

When water starts flowing into the capillary, initially filled with air, it detaches from the passage wall. The reason for this is that water upstream of the capillary inlet gains a considerable momentum along the top surface of the orifice. This momentum does not allow the flow to perfectly follow the sudden 90-degree turn of the wall. Figure 5 shows the frontline of water jet as it enters the capillary at different instants of time, for a type-1 orifices at Reynolds number of $Re = 116190$ ($p = 300$ MPa). Detachment of the flow right after the 90-degree corner is clear. It can be seen (Figure 5a) that after about 0.05 microseconds, the water front enters the capillary section. Note also that the flow passes the capillary section without reattaching to the capillary wall (Figure 5a-h). This is because the Reynolds number is so high that the flow takes a longer distance before it loses its kinetic energy. Therefore it clear passes the capillary section. Since we do not have reattachment, air freely circulates and envelops the jet avoiding jet instability arising from wall friction. This fact results in longer break-up length. A zoomed velocity vector in the capillary shows air circulation (Figure 6). On the other hand, simulation of the flow in type-2 orifices reveals that even for the lowest considered Reynolds number (10 MPa), there is

detachment of the flow at the entrance because the flow momentum along the top horizontal surface of the orifice is enough to separate the flow from the vertical capillary wall. However, this is followed by reattachment.

3.3 Effects of orifice geometry on reattachment length

The above discussion of the results of the jet formation of type-1 and type 2 orifices at high injection pressures evidenced that the reattachment length varies with the orifice internal geometry. It is important to study the reattachment length of the flow inside the two orifice types. The reattachment length is a function of the inlet diameter, inlet corner radius and flow Reynolds number. For the case of a sharp inlet, the flow at different pressures was simulated and the reattachment length was calculated for the two types of orifices (type-1 and type-2). To achieve a range of reattachment lengths at the considered injection pressures, the aspect ratio (*AR*) of the orifice type-1 has been changed now onwards to the value of 1.5 Figure 7 shows the reattachment lengths of water jets in a sharp-edge cone-capillary type-1 orifice at different injection pressures.

The moment that reattachment occurs can be determined by a sudden increase (2 to 3 orders of magnitude) in the flow density in the cells adjacent to the wall, which is initially equal to the density of air. For even the lowest considered injection pressure, there is detachment at the entrance to the orifice. Increasing the Reynolds numbers slightly increases the reattachment length. Further increasing the Reynolds number did not show any significant change in the reattachment length of type-2 orifice. The reattachment lengths normalized by the capillary diameter are plotted for type-1 and type-2 orifices in Figure 8. It can be seen that (l_r /d = 0.7) seems to be as an upper limit for the reattachment length for type-2 orifices, whereas it increased with injection pressure for type-1 orifice. The flow of type-2 orifice is a cavitating flow. Air is entrapped between the jet and the wall forming air ring. Break-up of the air ring and its dispersion, in cavitating nozzles, causes a great amount of disturbance and turbulence which perturbs the integrity and collimation of the forming water jet [1]. Simulations of the orifice type-1 with *AR* = 0.6 gave no reattachment (i.e. cavitation free constricted water jet) at all considered injection pressures. With increase of the capillary length of the type-1 orifice, it is possible to simulate the reattachment which occurs some where downstream at a distances beyond the *AR* =0.6 limit. We run a simulation of a flow in type-1 orifice with (*AR* = 1.5). As can be seen in figure 7, the reattachment length generally increased with increasing the injection pressure. The reattachment lengths for the two types of orifices normalized by their respective capillary diameter are plotted in Figure 8. Note that the minimum reattachment length for orifice type-1 is 0.64 which is still greater than its real aspect ratio (i.e. 0.6). Since there is no reattachment in type-1 orifice with (*AR*=0.6) at all considered injection pressures, we avoid problems of cavitation formation and collapse. As a result, the water jet stays laminar and glassy for significant distance downstream the orifice. The results shown in Figure 8 indicate that the critical capillary length for which an orifices is producing a cavitations free constricted water jet is a function of the orifice internal geometry. It can be seen that a constricted laminar jet is formed without any disturbances induced from the walls for type-1 orifices. On the other hand, orifice type-2 produced a cavitating flow.

If the capillary length is smaller than the reattachment length like in type-1 orifice, the orifice can be more resistant against instabilities in waterjet operation. These instabilities, which can be observed in the form of considerable fluctuations in the break-up length of the jet, may occur because of the structural vibration and/or flow pulsation. Such disturbances can cause a detached flow to reattach to the wall and cause cavitation.

The difference in the performance in terms of reattachment length for the two types of orifices are consistent with there applications: orifice type-1 is used in a pure water jet cutting applications. Therefore, the jet coherence (long break-up length) and momentum collimation are more important for cutting efficiency and accuracy. Whereas for type-2 orifices, the coherence of the jet serves little. Ruther the higher discharge coefficient is useful for better mixing of the abrasive particles and the water jet in the mixing head.

4-CONCLUSIONS

The flow through a type-1 and type-2 water jet orifice at real water jet pressures was simulated. Simulation and experimental discharge coefficients and centreline velocity magnitude were compared to validate the simulation. A good agreement was found. The discharge coefficients for type-1 orifice were found to be about 0.61 and stayed the same until the steady-state condition was reached. However, the discharge coefficient in the type-2 orifice, changed from about 0.61 to 0.93 with time as the fluid flowed through the capillary (unsteady-state condition). This condition indicates flow reattachment which can be followed by orifice cavitations. The results are found to be consistent and relevant to the application of each orifice types. The role of the orifice geometry in the formation of constricted and non-constricted water jets were discussed along with their importance and characteristics. In particular, the formation of constricted water jet through a sharp-edged orifice was simulated and the flow reattachment lengths at real water jet injection pressures were reported. It is concluded that ($l_r / d = 0.7$) seems to be an upper limit for the reattachment length for type-2 orifices which produced reattached flow (cavitating) for all considered injection pressures. Whereas, the type-1 orifice produced a cavitation-free constricted jet for all considered injection pressures. This certainly is favourable for pure water jet cutting process compared to a constricted water jet which are formed if the nozzle undergoes a hydraulic flip; because in the later case the jet first cavitate (atomizes) and then turns into a laminar long intact-length stream. Further conclusion is that, for obtaining a cavitation-free constricted water jet, the capillary length should be less than a critical length. For type-1 and type-2 orifices the critical capillary length is found to be about 100% (for typical pure water jet cutting) and 70% of their diameters respectively. It was also demonstrated that if the capillary length is less than the critical length, water jet is less prone to reattachments that may be caused due to system vibration or flow pulsation. Moreover, the cavitation-free orifices are not exposed to cavitation damages and will potentially have a greater lifetime. Further developments of the present study will investigate on the effect of orifice geometry on cutting performances.

5-ACKNOWLEDGMENTS

6-REFERENCES

1. Akira Sou, Shigeo Hosokawa, Akio Tomiyama, "Effects of cavitation in a nozzle on liquid jet atomization" *Int.l Journal of heat and mass transfer*, Vol. 50, No.17-18, 2007, pp. 3575-3582.
2. Tamaki, N., Shimizu, M., and Hiroyasu, H., "Enhancement of the atomization of a liquid jet by cavitation in a nozzle hole," *Atomization and Sprays*, Vol. 11, No. 2, 2001, pp. 125.
3. Hiroyasu, H., "Spray breakup mechanism from the hole-type nozzle and its applications", *Atomization and Sprays*, Vol. 10, No. 3-5, 2000, pp. 511-527.
4. Tafreshi, H. and Pourdeyhimi, B., "Simulating cavitation and hydraulic flip inside hydroentangling nozzles," *Textile Research Journal*, Vol. 74, No. 4, 2004, pp. 359-364.
5. H. Chaves, et al., "Experimental Study of Cavitation in the Nozzle Hole of Diesel Injectors Using Transparent Nozzles," *SAE Paper No. 950290*, pp. 199-211, 1995.
6. N. Anantharamaiah, H. Vahedi Tafreshi, and B. Pourdeyhimi,(2001) "Numerical Simulation of the Formation of Constricted Waterjets in Capillary Nozzles: Effects of Nozzle Geometry" *Chemical Engineering Research and Design*, 84 (A3), pp. 231-238
7. Hashish, M. "Pressure effects in abrasive-waterjet (AWJ) machining." *Trans. of the ASME, J. of Engineering Materials and Technology*, 1989, vol. 111, July, p. 221-228.
8. Vahedi Tafreshi H, Pourdeyhimi B. "The effects of nozzle geometry on waterjet breakup at high Reynolds numbers." Exp.t in Fluids (2003) 35:364–371
9. Lin, S.P., Reitz, R.D. "Drop and spray formation from a liquid jet", *Annual Review of Fluid Mechanics*, 30, (1998)
10. McCarthy, J., and Molloy, N.A., "Review of Stability of Liquid Jets and the Influence of Nozzle Design", *The Chemical Engineering Journal*, Vol. 7, PP. 1-20, (1974)
11. Reitz, R.D., and Bracco, F.V., "Mechanism of Atomization of a Liquid Jet, *Phys. of Fluids*, 25(10), (1982)
12. Ruiz, F., and Chigier, N., "The Mechanics of High Speed Atomization", *Proc. 3rd Iclass-85*, London, England, July 8-10, 1985. Volume 1 (A87-13826 03-34). London, Institute of Energy, p. VIB/3/1-VIB/3/15, (1986)
13. Rayleigh, L. "On the Instability of Jets", Proc. London Math. Soc., 10, pp. 4–13, (1879b)
14. M. Annoni, M. Monno "Effects of diamond orifice geometry on water jet cutting performance" 18th international conference on water jetting, Sept. 13-18, 2006 Gdansk, Poland,
15. Begenir, A., Vahedi Tafreshi, H., and Pourdeyhimi, B., 2004, "Effects of the Nozzle Geometry on Hydroentangling Waterjets: Experimental Study." *Textile Research Journal,* 74(2), 178-184.
16. Patankar, S.V., 1980, Numerical Heat Transfer and Fluid Flow. Washington DC: Hemisphere.
17. Fluent, 2002 FLUENT 6 user guide, 2002
18. Hirt, C.W.; Nichols, B.D. (1981), "Volume of fluid (VOF) method for the dynamics of free boundaries", *Journal of Computational Physics* 39 (1),
19. Youngs, D. L., 1982, "Time-Dependent Multi-Material Flow with Large Fluid Distortion, in Morton, K.W., & Baines, M.J., editors, Numerical Methods for Fluid Dynamics, Academic Press.
20. Brackbill, J.U., Kothe, D.B., & Zemach, C., 1992, "A Continuum Method for Modeling Surface Tension." J. Comput. Phys., 100, 335-354.
21. Wu, P.K., Miranda, R. F. & Faeth, G.M., 1995, "Effects of initial flow conditions on primary breakup of non-turbulent and turbulent round liquid jets." *Atomization and sprays,* 5, 175-196.

22. Ghassemieh, E., Versteeg, H.K. & Acar, M., 2003, "Effect of Nozzle Geometry on the Flow Characteristics of Hydroentangling Jets." *Textile Research Journal*, 73(5), 444-450.

7-NOMENCLATURE

ρ density, kg.m-3

$\bar{v}$ velocity vector, m.s-1

$\bar{g}$ gravitational acceleration, m.s-2

t time, s

$\overline{F}$ external body forces, N

μ molecular viscosity, Pa.s

α_q q^{th} fluid's volume fraction

F_{vol} volume force or force at the surface, N.m-3

σ surface tension, N.m-1

κ surface curvature, m-1

n unit vector normal to the plane

Re Reynold number based on capillary diameter

p injection pressure, MPa

l length of capillary section of orifice, mm

l_r reattachment length of the water jet, mm

L_t length of the strip thikness

d diameter of the orifice inlet, mm

AR Aspect ratio (l/d)

Ψ Cone angle (degree)

Subscripts

0   orifice entry section

1   orifice exit section

th   theoretical

sim.   simulation

exp.t   experimental

8-TABLES

Table 1: Main geometrical characteristics of the diamond orifices (other dimensions are confidential information)

Conventional name	Type-1 (AWJ)	Type-2 (WJ)
Diameter (d)	0.25	0.15
Aspect ratio (AR)	1	0.6
Cone angle (ψ)	30^0	60^0

9-GRAPHICS
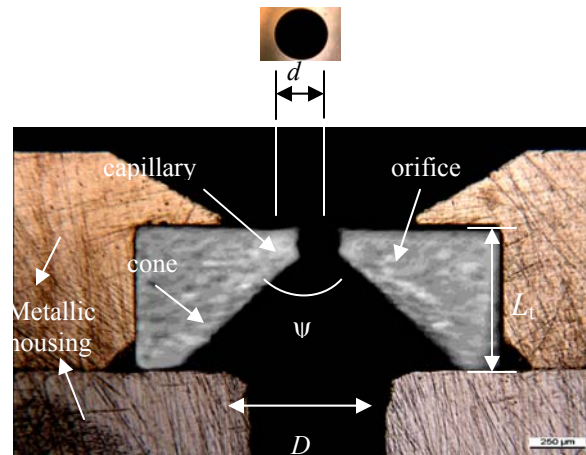
Figure 1: A typical waterjet machining orifice. Capillary diameter, $d \approx 150\mu m$, cone base diameter $D \approx 500$ μm. Strip thickness, L_t, is 0.5 mm, and $AR = 1$.
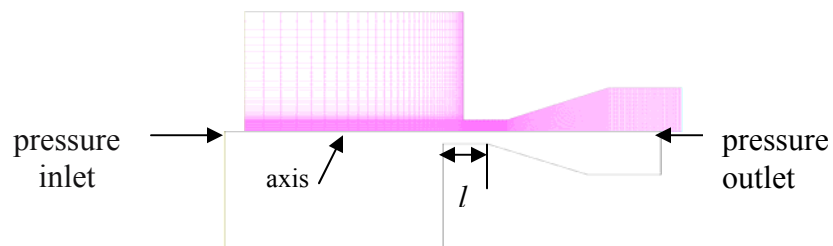
Figure 2: Simulation domain and boundary conditions along with mesh distribution in the capillary section of the orifice.
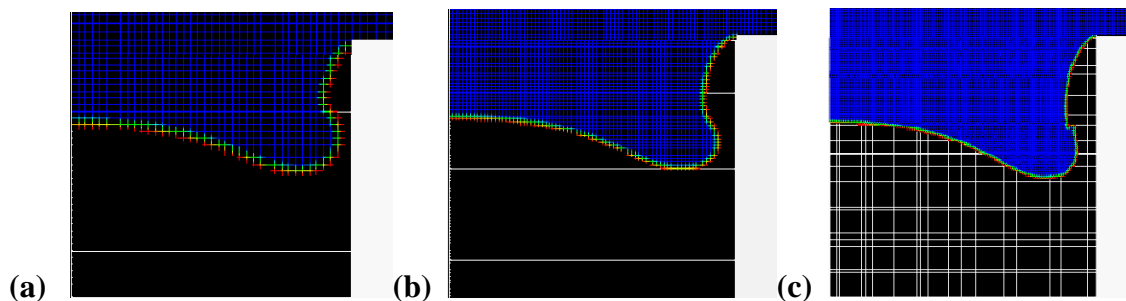
Figure 3. Simulations performed in an axi-symmetric geometry applyingthe following mesh densities along the radial and axial directions inside the capillary are (a): 40 × 80, (b): 80 ×160, and (c): 160 × 320.
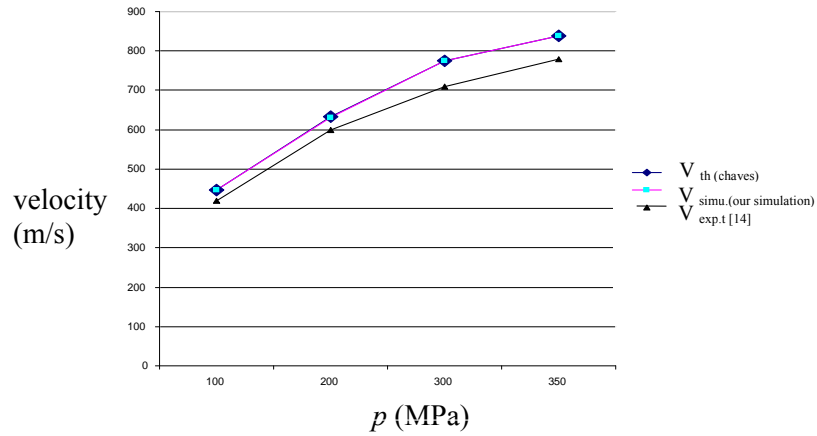
Figure 4. Simulated (at 1 mm from the orifice exit) and experimental (at 22 mm from the orifice exit) velocity magnitudes.
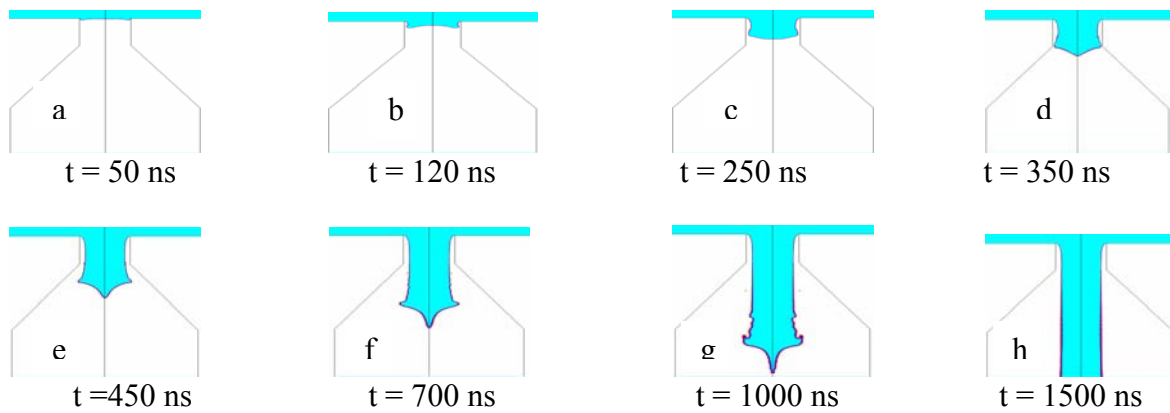
Figure 5. Different times during water flow into an initially air-filled cone-capillary nozzle. Detached Flow and the formation of constricted water jet can be seen at $Re = 116190$ ($p = 300$MPa).
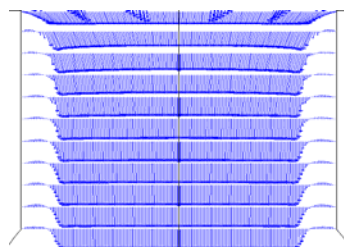
Figure 6. Velocity vectors in the capillary show air circulation.

| p =10 MPa | p =20 MPa | p =50 MPa | p =100 MPa | p =200 MPa |
| p =300 MPa | p =400 MPa | p = 500 MPa | p = 600 MPa | p = 700 MPa |
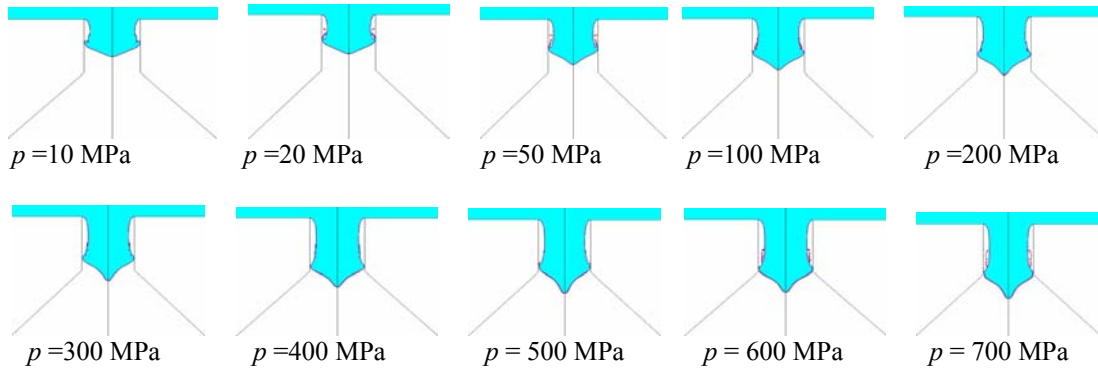
Figure 7: Water flow into a type-1 orifice with *AR* = 1.5 at different injection pressures. Each picture shows the moment of reattachment at the given injection pressure.
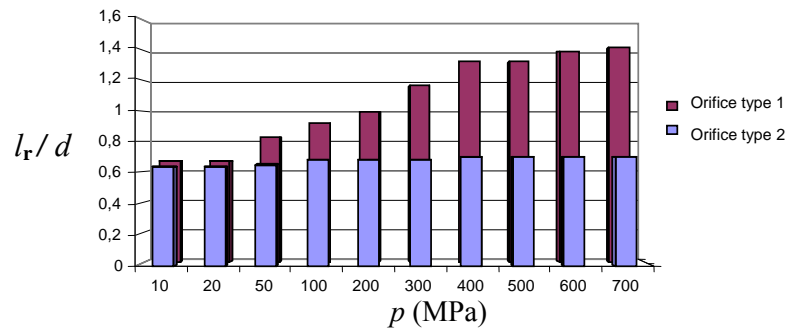
Figure 8. Normalized reattachment length versus injection pressure for a sharp-edge cone capillary orifice (type-1 and type-2).